Tuning Pore Heterogeneity in Covalent Organic Frameworks for Enhanced Enzyme Accessibility and Resistance against Denaturants

Qi Sun, Briana Aguila, Pui Ching Lan, and Shengqian Ma*

Achieving high-performance biocomposites requires knowledge of the compatability between the immobilized enzyme and its host material. The modular nature of covalent organic frameworks (COFs), as a host, allows their pore geometries and chemical functionalities to be fine-tuned independently, permitting comparative studies between the individual parameters and the performances of the resultant biocomposites. This research demonstrates that dual pores in COFs have profound consequences on the catalytic activity and denaturation of infiltrated enzymes. This approach enforces a constant pore environment by rational building-block design, which enables it to be unequivocally determined that pore heterogeneity is responsible for rate enhancements of up to threefold per enzyme molecule. More so, the enzyme is more tolerant to detrimental by-products when occupying the larger pore in a dual-pore COF compared to a corresponding uniform porous COF. Kinetic studies highlight that pore heterogeneity facilitates mass transfer of both reagents and products. This unparalleled versatility of these materials allows many different aspects to be designed on demand, lending credence to their prospect as next-generation host materials for various enzyme biocomposites catalysts.

Enzymes are remarkable natural catalysts capable of manipulating a wide range of complex substrates with unparalleled selectivity.[1] To use nature's merits, protein engineering tools are being developed to make designer enzymes tailored for specific chemical transformations, giving biocatalysis a greater promise for a variety of industrial applications.[2] However, the utilization of cell-free enzymes thus far has been limited, in part due to deficiencies in stability, operating range, and recyclability. Approaches that yield comparably high activity and stability, while providing ancillary benefits, such as easy handling, transportation, and storage of enzymes, are therefore highly desirable.[3] Coupling enzymes with solid materials offer better opportunities to overcome these challenges, but the design of effective immobilization techniques still represents

Dr. Q. Sun, B. Aguila, P. C. Lan, Prof. S. Ma
Department of Chemistry
University of South Florida
4202 E. Fowler Avenue, Tampa, FL 33620, USA
E-mail: sqma@usf.edu

The ORCID identification number(s) for the author(s) of this article can be found under https://doi.org/10.1002/adma.201900008.

one of the main hurdles that continues to hamper the set-up of large-scale biocatalytic processes.[4,5] Among developed technologies, infiltrating enzymes within the pores of host materials open an auspicious pathway, offering promise in maintaining the enzyme's properties.[6] Nevertheless, given the divergent reaction outcomes of various biocomposites, fundamental elucidation of the host's pore chemistry, resulting in better enzymatic performance, is of critical importance in the design of efficient formulations.

Covalent organic frameworks (COFs) are porous crystalline polymers composed of organic units/molecules linked via covalent bonds, which present solutions to the aforementioned obstacles from a chemical and architectural perspective. The versatile synthesis of COFs allows the design and control of network topology, pore size, and chemical functionality, which can be exploited to study structure–function relationships.[7] Indeed, the enormous design adaptability of pore geometries and chemical functionalities, along with high specific internal surface areas make COFs highly desirable for catalysis,[8] optoelectronic devices,[9] environmental remediation,[10] and nanofiltration membranes,[11] among others.[12] These adjustable properties also facilitate their application in biological fields.[13] Their ability to design on demand enables high fidelity, with atomic precision of its chemical and structural features independently, thus elucidating the structure–function relationships of the biocomposite's performance. Previously, our research group has shown that an enzyme's performance can be systematically optimized by varying the pore environment of isostructural 2D COFs in the case of lipase PS.[14] The hydrophobic pore channels in the COF improved lipase activity by introducing a lid opening near the active site resulting in superior performance, compared to a MOF and mesoporous silica, both with higher hydrophilicities (Table S1, Supporting Information).

Although these COF-enzyme systems have been shown to protect the immobilized enzymes from deactivation and gave orders of magnitude higher catalytic activities relative to the free enzymes, there is still room for improvement when the following are taken into account: (i) blocked pores or partially blocked pores by the enzymes, and (ii) slow flux rates for

**ADVANCED
SCIENCE NEWS**

www.advancedsciencenews.com

**ADVANCED
MATERIALS**

www.advmat.de

reagents and products. To alleviate such transport limitations, it is highly desirable to reduce the diffusion path lengths. The preparation of hierarchical porous materials are among the versatile strategies adopted so far to provide a solution to such challenges.[15] In this contribution, we demonstrate that hierarchically porous COFs featuring two types of pores, hexagonal and triangular, can be utilized as ideal enzyme encapsulation platforms, whereby enzymes are loaded in hexagonal (larger) pore and reagents and products are free to ingress and egress in the triangular pores. The inimitable role of the hierarchical pore structure on the catalytic efficiency and robustness was delineated by comparing the enzymatic performance of these biocomposites using COFs with similar pore environments yet different pore structures. The enzyme encapsulated in dual-pore COFs outperforms that in the COFs with uniform porosity in terms of both activity and chemical resistance to by-products. This work provides a blueprint for the design of other porous materials geared toward improving the activity and stability of the enzyme as well as putting forth a promising design strategy in optimizing the performance of the encapsulated guest species.

In developing hierarchical COFs, an angle-specific vertex design strategy provides an effective synthetic method. A D_{2h} symmetric monomer, fourfold amine-functionalized tetraphenylethylene [4,4′,4″,4‴-(ethene-1,1,2,2-tetrayl)tetraaniline, ETTA], with two distinct angles (60° and 120°) between two adjacent arms has been demonstrated as a versatile vertex piece to design hierarchical nanoarchitectures.[16] To expand the

aperture of COF channels to be suitable for biomolecule admission, we employed a linear dialdehyde, 4,4′-(ethyne-1,2-diyl)dibenzaldehyde (EDDA) as the linking building unit. A mixture of ETTA and EDDA heated in the presence of a catalytic amount of 6 M acetic acid using 1,2-dichlorobenzene/n-butanol (1:1) as solvent resulted in the formation of the desired material (COF-ETTA-EDDA, **Figure 1**a). The Fourier transform infrared (FTIR) spectrum of COF-ETTA-EDDA was compared with that of the precursors and showed the appearance of an imine C=N stretch at 1620 cm⁻¹ with the concomitant disappearance of the aldehydic C—H and C=O stretching vibrations of EDDA and the N—H stretching vibrations of ETTA, indicative of the formation of the polymer network bonding moieties (Figure S1, Supporting Information).[17] To elucidate the structural features of the as-synthesized COF, powder X-ray diffraction (PXRD) analyses were performed. Its pattern was dominated by an intense reflection in the low-angle region, 2.0° of 2θ (Cu Kα1), attributed to the (100) facet of a primitive hexagonal lattice (Figure 1d, see also the enlarged figure in Figure S2 in the Supporting Information). Additionally, the presence of further weak reflections and a broad reflection at around 20° 2θ was assigned to the (001) facet, which corresponds to the π–π stacking in 2D crystalline COFs with a spacing of 4.8 Å (Figure 1b,c). In order to determine the periodic structure, a theoretical simulation was carried out using Materials Studio with subsequent refinement using the Forcite program (see structure simulation section). The reflections observed by experimental PXRD match well with the proposed AA-stacking mode of a dual-pore
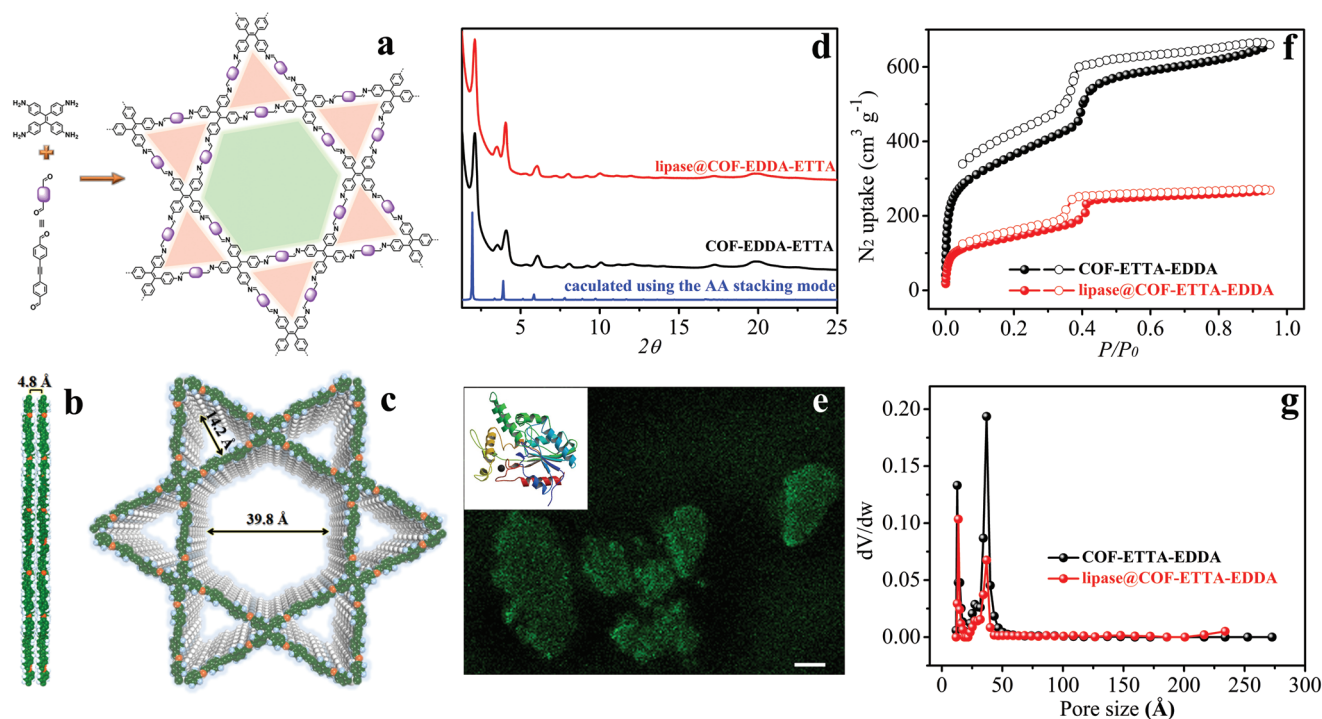
Figure 1. a) Synthetic scheme of COF-ETTA-EDDA through the condensation of 4,4′,4″,4‴-(ethene-1,1,2,2-tetrayl)tetraaniline (ETTA) and 4,4′-(ethyne-1,2-diyl)dibenzaldehyde (EDDA). b,c) Graphic view of AA-stacking mode of dual-pore Kagome structure of COF-ETTA-EDDA (green, C; orange, N; light blue, H). d) Calculated and experimental PXRD patterns. e) Confocal microscopy image of lipase@COF-ETTA-EDDA where lipase PS was labeled with fluorescein isothiocyanate (FITC), scale bar equals 10 µm, inset: graphic view of lipase PS. f,g) N₂ sorption isotherms collected at 77 K and corresponding pore size distribution based on the nonlocal density functional theory method.

**ADVANCED
SCIENCE NEWS**

www.advancedsciencenews.com

**ADVANCED
MATERIALS**

www.advmat.de

Kagome structure. Micro- and mesoporosity for COF-ETTA-EDDA were demonstrated by collecting nitrogen adsorption measurements at 77 K. The calculated Brunauer–Emmett–Teller (BET) surface area and total pore volume for this material were 1249 m^2 g^{-1} and 1.0 cm^3 g^{-1}, respectively (Figure 1f). DFT pore size distribution analysis revealed pore diameters of ca. 13.9 and 38.5 Å, assignable to the triangular micropores and hexagonal mesopores, respectively (Figure 1c,g). We reasoned that COF-ETTA-EDDA meets the criteria necessary as a promising enzyme carrier: (i) the large mesoporous channels (38.5 Å) are ideal for hosting enzymes and (ii) the narrower triangular channels effectively exclude biomolecules rendering them free to transport molecule-sized reactants and products. We selected lipase PS (dimensions of about 30 Å x 32 Å ingly flexible biocatalyst for a wide range of unnatural substrates and has been used industrially as detergent enzymes, in paper and food technology, thereby making them a preferred object for optimization.[17]

To immobilize the enzyme, COF-ETTA-EDDA was incubated with a phosphate buffer solution of lipase PS (30 mg mL^{-1}, pH = 7.0) at room temperature for 6 h followed by centrifugation and washing, affording the composite denoted as lipase@COF-ETTA-EDDA. The uptake capacity of lipase PS was determined by reverse quantification via quantifying the protein content in the supernatant by bicinchoninic acid (BCA) assay using UV–vis spectroscopy, showing that the loading capacity was 0.78 mg g^{-1} (see details in Experimental Section in the Supporting Information). FT-IR spectrum of lipase@COF-ETTA-EDDA indicates that the vibrational bands of the COF remain unaltered while additional lipase PS vibrations appear in the spectra of the enzyme loaded COF (Figure S3, Supporting Information). SEM images of COF-ETTA-EDDA did not indicate noticeable morphological changes following the enzyme uptake. This suggests that the enzyme does not reside on the outer surface of the COF nor does it form a separate phase, but rather occupies the COF's pores (Figure S4, Supporting Information). Energy-dispersive X-ray spectroscopy (EDX) analysis in a scanning transmission electron microscope (STEM) indicated that sulfur, a signature of the enzyme, is indeed located throughout the COF (Figure S5, Supporting Information). To provide additional proof for this claim, fluorescent probe fluorescein isothiocyanate (FITC) was used to label the enzyme molecules. From the confocal laser scanning microscopy (CLSM), it can be observed that FITC-lipase PS (green) is present throughout lipase@COF-ETTA-EDDA, underpinning the homogeneous accommodation of the enzyme in the crystalline framework (Figure 1d; Figure S6, Supporting Information).

PXRD analysis indicates that there is no significant difference with regard to the crystal structure between COF-ETTA-EDDA and lipase@COF-ETTA-EDDA samples, although decreased relative intensity of the peak assigned to the hexagonal pores was observed, attributable to a reduction in scattering contrast resulting from the inclusion of enzyme molecules in the mesopores of the COF (Figure 1d).[18] This was further confirmed by the N_2 sorption isotherm of lipase@COF-ETTA-EDDA, which showed a reduction in BET surface area to 497 m^2 g^{-1} (Figure 1f). The pore size distribution analysis of COF-ETTA-EDDA and lipase@COF-ETTA-EDDA indicates that the pore volume corresponding to the triangular channels of COF-ETTA-EDDA minimally drops from 0.13 to 0.10 cm^3 g^{-1}, whereas the incremental pore volume corresponding to the hexagonal channels greatly decreases from 0.19 to 0.06 cm^3 g^{-1} after lipase PS encapsulation (Figure 1g). We infer from these observations that lipase PS molecules should reside in the mesopores, while the micropores of 13.9 Å remain available. To allow analytes to transfer back and forth between micropores and mesopores we hypothesize that defects in the COF,[19] such as missing monomer connections, contribute to the improved performance. This will allow transfer through defects that are larger than the van der Waals space between COF layers which equates ≈1.4 Å. With only a single defect the space opens up to ≈6.2 Å allowing reactant and product diffusion.

To evaluate the enzymatic performance of lipase@COF-ETTA-EDDA, the kinetic resolution of racemic secondary alcohols was chosen with the considerations that the importance of enantiomerically pure alcohols and the highly enantioselective resolution activity of lipases.[20] The initial reactions were conducted using hexane as the medium with 1-phenylethanol and vinyl acetate as the acyl donor in the presence of the biocomposite (Figure 3a), given that a nonpolar medium benefits the performance of lipase PS (Table S1, Supporting Information).[14] To distinctly analyze the effect of the pore structure of the host materials on the catalytic properties of the enzymes, side-by-side comparisons were made with the enzyme infiltrated in a COF bearing a uniform pore structure with similar pore aperture and environment to the mesopore in COF-ETTA-EDDA. This material was synthesized by condensation of 4,4′,4″,4‴-(pyrene-1,3,6,8-tetrayl)tetraaniline (PY) with EDDA (**Figure 2**a) and then lipase PS was immobilized as described above (lipase@COF-PY-EDDA). PXRD patterns and computer modeling studies, together with pore size distribution analysis revealed that this material has high crystallinity and 1D square channels, with a diameter of 31.4 Å, along the c-axis (Figure 2b). The specific surface area was determined to be 1079 m^2 g^{-1}, which was reduced to 590 m^2 g^{-1} after enzyme loading (uptake capacity of 0.65 mg g^{-1}, Figure 2c). Detailed characterizations are given in Figures S7–S11 in the Supporting Information.

As displayed in **Figure 3**b, compared to the poor activity of the free enzyme, a drastically enhanced activity was observed after infiltrating in COF-PY-EDDA, revealing that immobilization can increase the accessibility of the active site of the enzyme, mainly due to the insoluble nature of lipase PS in hexane. Impressively, lipase@COF-ETTA-EDDA exhibits a further improvement in activity, about 1.5 times higher than that of lipase@COF-PY-EDDA, with the same enzyme content. Given the fact that these biocomposites possess very similar surface areas and pore environment of the host materials, the observed divergent reaction outcomes thereby suggest a role of the material's architecture in mass transfer.

To provide a more comprehensive comparison about the immobilized enzymes in COFs with different pore structures, we investigated the kinetic parameters. For each enzymatic reaction, the dose-dependent plots show that at high 1-phenylethanol concentrations, a plateau response is obtained, which is a characteristic of the Michaelis–Menten kinetic mechanism

ADVANCED
SCIENCE NEWS
www.advancedsciencenews.com

ADVANCED
MATERIALS
www.advmat.de
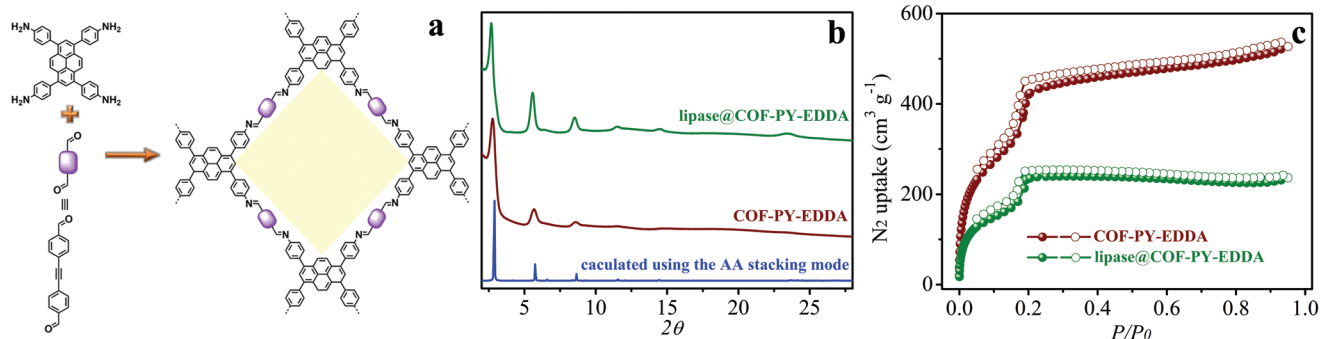
Figure 2. a) Synthetic scheme of COF-PY-EDDA through the condensation of 4,4′,4″,4‴-(pyrene-1,3,6,8-tetrayl)tetraaniline (PY) and 4,4′-(ethyne-1,2-diyl)dibenzaldehyde (EDDA). b) Calculated and experimental PXRD patterns, inset: graphic view of the eclipsed AA stacking structure of COF-PY-EDDA (green, C; orange, N; light blue). c) N$_2$ sorption isotherms collected at 77 K.

(Figures S12 and S13, Supporting Information). According to the Lineweaver–Burk Equation (1)

$$\frac{1}{V} = \frac{K_m}{V_{max}}\frac{1}{[S]} + \frac{1}{V_{max}} \tag{1}$$

Where V is the initial velocity, V_{max} represents the maximal reaction velocity, $[S]$ corresponds to the concentration of the substrate, and K_m is the Michaelis constant, the parameters of the reaction kinetics of the enzymes encapsulated within different pore structure materials, including the apparent Michaelis–Menten constant (K_m), and maximum reaction rate (V_{max}) are summarized in **Table 1** (see also Figures S12 and S13 in the Supporting Information). The K_m is a reflection of the enzymatic affinity for a substrate, and a high K_m value represents a weak affinity and vice versa. In addition, the rate parameter k_{cat}/K_m, where k_{cat} refers to the catalytic reaction rate constant, can be used to monitor the enzymatic reaction. Compared with the enzymes immobilized in the dual-pore COF, those in the single pore COF-PY-EDDA show a relatively smaller k_{cat} value, but larger K_m value, and thereby smaller k_{cat}/K_m, which demonstrates that lipase PS molecules in COF-ETTA-EDDA are more efficient. Given that COF-PY-EDDA contains only square mesoporous channels, this result is not surprising because many of the mesopores are expected to be occupied by encapsulated enzymes, leaving limited room for reactant diffusion.

To further illustrate the benefit of hierarchically porous COFs as an appealing platform for enzyme encapsulation and to show the geniality of this observation, another dual-pore COF material (COF-ETTA-DMDA, BET: 952 m^2 g^{-1}, **Figure 4**a) and corresponding single pore analogue (COF-TPB-DMTP, BET: 1740 m^2 g^{-1}, Figure 4b) were synthesized for comparison. The detailed characterizations of these materials are shown in Figures S14-S18 and Table S2 in the Supporting Information. Again, the enzymes infiltrated in the dual-pore COF were kinetically favored compared to those in its single pore analogue (Figure 3c). Specifically, lipase@COF-ETTA-DMDA and lipase@COF-TPB-DMTP afforded an initial reaction rate of
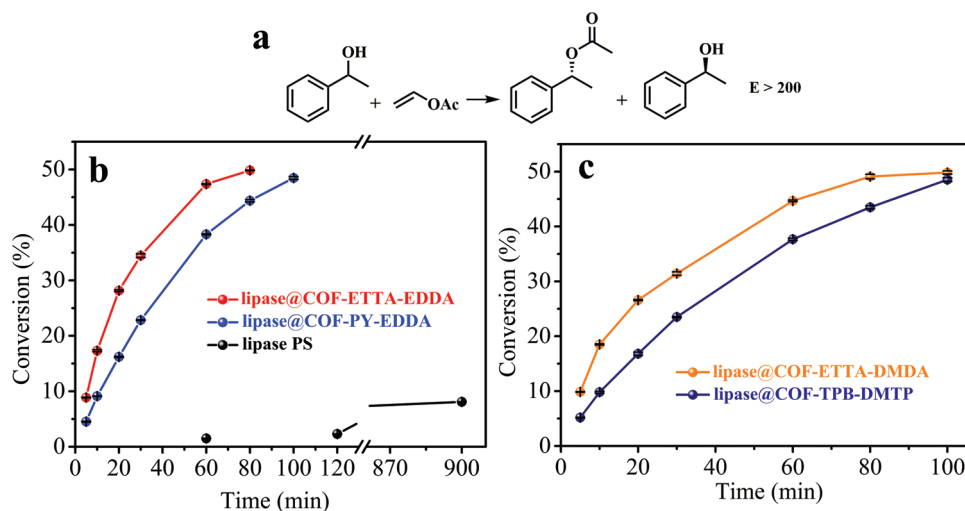
Figure 3. Catalytic performance comparison. a) Reaction equation. b,c) Conversion plots of kinetic resolution of 1-phenylethanol with vinyl acetate as the acyl donor over free lipase PS and various biocomposites. Reaction conditions: 1-phenylethanol (1.0 mmol), vinyl acetate (3.0 mmol), hexane (4.0 mL), and 45 °C in the presence of free lipase PS (2.5 mg) or biocomposites with the same content of lipase PS (2.8 mg of lipase@COF-ETTA-EDDA, 3.4 mg of lipase@COF-PY-EDDA, 3.6 mg of lipase@COF-ETTA-DMDA, or 2.5 mg of lipase@COF-TPB-DMTP, all with a lipase PS content of 1.2 mg. For a summary lipase PS loading capacities in various COF materials and textural parameters of these materials see also details in Table S2 in the Supporting Information).

Table 1. Comparison of kinetic parameters for lipase PS immobilized into COFs with various pore structures.

COFs	K_m [mM]	V_{max} [mM min^{-1}]	V_{max}/K_m [min^{-1}][a]
COF-ETTA-EDDA	0.3315	0.665	2.001
COF-PY-EDDA	0.4017	0.112	0.279

[a]V_{max}/K_m used as a reflection of k_{cat}/K_m, due to similarity in enzyme amount in each COF and volume of reaction system, where $k_{cat} = V_{max}/[E]$ and $[E]$ represents the concentration of the enzyme.

9.8 mM min^{-1} and 5.2 mM min^{-1}, respectively, with the same enzyme contents. Taking into account that the biocomposite with higher surface area did not afford superior performance, further accentuates the importance of pore structure to augment the utilization efficiency of the encapsulated enzymes. Together with previous reports, this observation demonstrates that specific surface area (as measured by N$_2$ isotherms) is not always an accurate indicator of the accessibility of the active sites on the heterogeneous catalysts. Rather, the material's pore structure is more influential on the catalytic rate. Following the enzyme uptake by the mesoporous channels, the microporous channels of the hierarchically structured host material remain open and available as conduits for reactant and product diffusion to and from the active sites of the encapsulated enzymes, facilitating internal diffusion of reactants to reach the enzyme sites.

After such encouraging results for the enzyme infiltrated in dual pore COFs, we became interested in investigating whether this behavior could be used to stabilize enzymes by eliminating side products, which are known to cause deactivation. Given the increasing demand of biodiesel and high specificity of lipases in comparison with other conventional chemical catalysts employed in industrial biodiesel production,[21] the transesterification of triacylglycerides to fatty acid ethyl esters, as exemplified by the reaction between bean oil and ethanol, was chosen as a proof-of-concept case (**Figure 5**a), with the knowledge that they typically suffer from product inhibition. In this reaction, the by-product glycerol can cause clogging of the immobilized enzymes, thereby preventing the reactant from accessing the active sites, which leads to severe deterioration in process performance. We reasoned that if glycerol can be

efficiently expunged from the active sites, the aforementioned concerns are expected to be addressed.

To our delight, consistent with our hypothesis, the enzymatic activity of lipase PS in transesterification was significantly enhanced by encapsulation in hierarchically porous COFs compared to that in the COFs with uniform porosity. Only 11% of the product was detected in the presence of lipase PS after 3 h, whereas a full conversion of triacylglycerides was achieved for lipase@COF-ETTA-EDDA within 1 h, under otherwise identical conditions. Notably, the rate of bean oil transesterification by lipase@COF-ETTA-EDDA is around three times that of lipase@COF-PY-EDDA and no product was detected if only COFs were used (Figure 5b). Moreover, the initial transesterification rate of lipase@COF-PY-EDDA drops by around twofold when it was reused after a brief washing with hexane. Upon closer examination of the reaction profile for the second cycle, we observed a 10 min induction period time, which suggests that substrates/products were retained within the pores and blocked new substrates from entering. To provide evidence, we extracted the catalyst with ethanol after the first cycle, given the immiscibility between hexane and glycerol. Indeed, a significant amount of the entrapped glycerol was observed and the induction period was eliminated, but the catalytic activity of the extracted material still was not fully restored, probably due to the denaturation of the enzymes after prolonged exposure to glycerol (see details in the enzymatic activity assay section in the Supporting Information). By contrast, the catalytic activity of the reused lipase@COF-ETTA-EDDA was comparable to its initial level and less glycerol was found to be trapped in lipase@COF-ETTA-EDDA after reaction.

To reveal the underlying reasons behind the observed phenomenon and to determine the dominant mechanism of glycerol inhibition in transesterification, reactions with added glycerol were carried out. The results in Figure 5c show that the added glycerol had little effect on the activity of the biocomposites and around 90% catalytic activities were retained for both lipase@COF-ETTA-EDDA and lipase@COF-PY-EDDA with varying additions of external glycerol. This indicates that the impact of glycerol as a competing substrate is negligible when glycerol and ethanol coexist. This experiment thus verifies that the mechanism of inhibition is mainly caused by by-product glycerol clogging the pores of the catalyst.
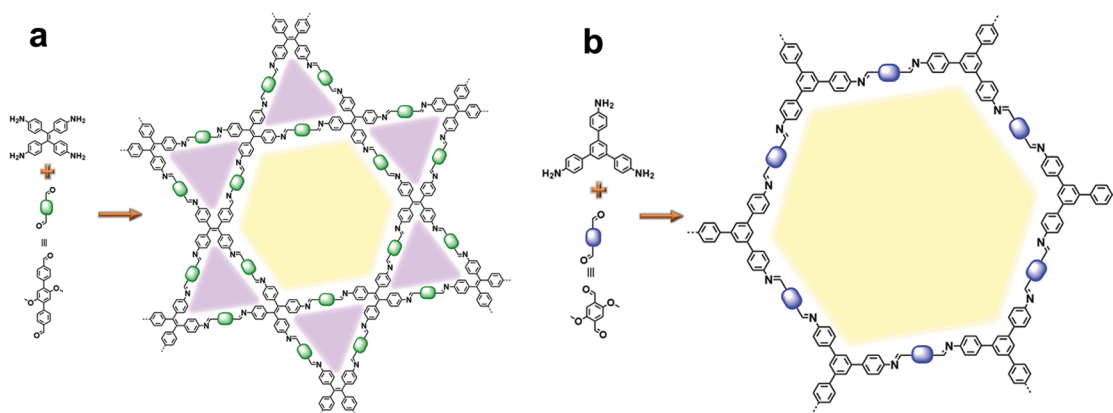
Figure 4. a,b) Synthetic schemes of COF-ETTA-DMDA (a) and COF-TPB-DMTP (b).

**ADVANCED
SCIENCE NEWS**
www.advancedsciencenews.com

**ADVANCED
MATERIALS**
www.advmat.de
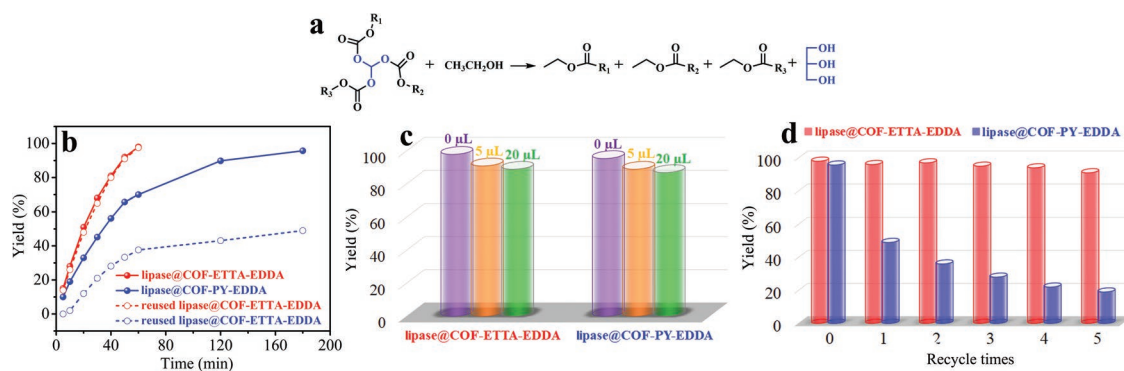
Figure 5. a) Catalytic performance comparison between lipase@COF-ETTA-EDDA and lipase@COF-PY-EDDA in the transesterification of triacylglycerides to fatty acid ethyl esters. b) Fatty acid ethyl esters yield verse time plots. c) Glycerol sensitivity tests. d) Recycling tests. Reaction conditions: soybean oil (20 mg), ethanol (100 µL), lipase@ETTA-EDDA (2.8 mg), or lipase@COF-PY-EDDA (3.4 mg), and 40 °C.

To gauge the significance of a dual-pore structure for mass transfer and to support the low glycerol retention of lipase@COF-ETTA-EDDA, thereby enhancing the durability of the catalyst, we compared the activities of lipase@COF-ETTA-EDDA and lipase@COF-PY-EDDA at a low catalyst loading. Time-dependent conversion curves indicated that the reaction catalyzed by lipase@COF-ETTA-EDDA was superior to that catalyzed by lipase@COF-PY-EDDA. It is shown that lipase@COF-PY-EDDA was deactivated at approximately 60% conversion, and prolonging the reaction time only lead to negligible additional product formation, suggesting the accumulation of glycerol around the enzyme and thereby preventing the bean oil access. In striking contrast, the yield steadily increased over time in the presence of lipase@COF-ETTA-EDDA and the product yield was higher than 99.0% within 5 h (Figure S19, Supporting Information). These results further demonstrate the importance of pore structure in enhancing the diffusion of reactant/product. The formed glycerol could be excluded instantaneously from lipase@COF-ETTA-EDDA, resulting in negligible bound glycerol and therefore no catalyst clogging and greater durability.

The robustness of lipase@COF-ETTA-EDDA was further validated through recycling experiments. Upon conclusion of the reaction, lipase@COF-ETTA-EDDA was isolated by centrifugation and washed several times with hexane before being dried under vacuum. The transesterification reaction was then performed again under identical conditions. The activity of lipase@COF-ETTA-EDDA remained, without a significant decrease in the efficiency of the catalyst or structural deterioration as determined by PXRD analysis (Figure 5d; Figures S20 and S21, Supporting Information), after more than five consecutive cycles. To further probe the effect of pore structure on the catalyst recyclability, we evaluated the multiuse performance of lipase@COF-PY-EDDA. Again, this recyclability further demonstrates the outperformance of hierarchically porous COFs versus those with uniform pore structures (Figure 5d).

In conclusion, our results demonstrated that COFs are a viable scaffold for enzyme immobilization, which meet the requirements for practical applications. The enzyme immobilized in dual-pore COFs is characterized by superior reactant accessibility and higher activity, as well as greater resistance to detrimental by-products and denaturants than does the same enzyme encapsulated in COFs with uniform pore structures. Presuming this phenomenon to be general, these findings suggest structure–property correlation design rules for hierarchical pore structuring of host frameworks for enzyme-encapsulation applications. The dual-pore COFs presented herein are the first to be investigated in this context, representing an unexplored field of applications for COFs. Given the enormous diversity of molecular building units that can be employed in the construction of COFs, both the development of new framework structures and fine-tuning the properties of existing ones are possible, enabling the modulation of enzymatic activity to be rigorously controlled. We envision that future research on studying the building blocks' properties and stacking modes together will allow for further optimization of enzymatic performance, long-term durability, and recyclability in order to provide off-the-shelf enzyme catalysts.

Supporting Information

Supporting Information is available from the Wiley Online Library or from the author.

Acknowledgements

Conflict of Interest

The authors declare no conflict of interest.

Keywords

[1] a) A. J. J. Straathof, *Chem. Rev.* **2014**, *114*, 1871; b) L. M. Podust, D. H. Sherman, *Nat. Prod. Rep.* **2012**, *29*, 1251.

[2] a) C. K. Prier, R. K. Zhang, A. R. Buller, S. Brunkmann-Chen, F. H. Arnold, *Nat. Chem.* **2017**, *9*, 629; b) H. E. Schoemarker, D. Mink, M. G. Wubbolts, *Science* **2003**, *299*, 1694; c) H. S. Toogood, N. S. Scrutton, *ACS Catal.* **2018**, *8*, 3532.

[3] A. Schmid, J. S. Dordick, B. Hauer, A. Kiener, M. Wubbolts, B. Witholt, *Nature* **2001**, *409*, 258.

[4] a) R. Dicosimo, J. McAuliffe, A. J. Poulose, G. Bohlmann, *Chem. Soc. Rev.* **2013**, *42*, 6437; b) U. Hanefeld, L. Gardossi, E. Magner, *Chem. Soc. Rev.* **2009**, *38*, 453; c) Z. Zhou, M. Hartmann, *Chem. Soc. Rev.* **2013**, *42*, 3894; d) U. T. Bornscheuer, *Angew. Chem., Int. Ed.* **2003**, *42*, 3336; e) R. A. Sheldon, *Adv. Synth. Catal.* **2007**, *349*, 1289.

[5] a) X. Lian, Y. Fang, E. Joseph, Q. Wang, J. Li, S. Banerjee, C. Lollar, X. Wang, H.-C. Zhou, *Chem. Soc. Rev.* **2017**, *46*, 3386; b) M. B. Majewski, A. J. Howarth, P. Li, M. R. Wasielewski, J. T. Hupp, O. K. Farha, *CrystEngComm* **2017**, *19*, 4082; c) C. Doonan, R. Riccò, K. Liang, D. Bradshaw, P. Falcaro, *Acc. Chem. Res.* **2017**, *50*, 1423; d) E. Gkaniatsou, C. Sicard, R. Ricoux, J.-P. Mahy, N. Steunou, C. Serre, *Mater. Horiz.* **2017**, *4*, 55; e) W.-H. Chen, M. Vázquez-González, A. Zoabi, R. Abu-Reziq, I. Willner, *Nat. Catal.* **2018**, *1*, 689; f) Q. Wang, X. Zhang, L. Huang, Z. Zhang, S. Dong, *Angew. Chem., Int. Ed.* **2017**, *56*, 16082; g) F.-K. Shieh, S.-C. Wang, C.-I. Yen, C.-C. Wu, S. Dutta, L-Y. Chou, J. V. Morabito, P. Hu, M.-H. Hsu, K.-C.-W. Wu, C.-K. Tsung, *J. Am. Chem. Soc.* **2015**, *137*, 4276; h) Y. Pan, H. Li, J. Farmakes, F. Xiao, B. Chen, S. Ma, Z. Yang, *J. Am. Chem. Soc.* **2018**, *140*, 16032; i) F. Lyu, Y. Zhang, R. Z. Zare, J. Ge, Z. Liu, *Nano Lett.* **2014**, *14*, 5761.

[6] a) V. Lykourinou, Y. Chen, X.-S. Wang, L. Meng, T. Hoang, L.-J. Ming, R. L. Musselman, S. Ma, *J. Am. Chem. Soc.* **2011**, *133*, 10382; b) D. Feng, T.-F. Liu, J. Su, M. Bosch, Z. Wei, W. Wan, D. Yuan, Y.-P. Chen, X. Wang, K. Wang, X. Lian, Z.-Y. Gu, J. Park, X. Zou, H.-C. Zhou, *Nat. Commun.* **2015**, *6*, 5979; c) H. Deng, S. Grunder, K. E. Cordova, C. Valente, H. Furukawa, M. Hmadeh, F. Gándara, A. C. Whalley, Z. Liu, S. Asahina, H. Kazumori, M. O'Keeffe, O. Terasaki, J. F. Stoddart, O. M. Yaghi, *Science* **2012**, *336*, 1018; d) P. Torres-Salas, A. del Monte-Martinez, B. Cutiño-Avila, B. Rodriguez-Colinas, M. Alcalde, A. O. Ballesteros, F. J. Plou, *Adv. Mater.* **2011**, *23*, 5275; e) E. Gkaniatsou, C. Sicard, R. Ricoux, L. Benahmed, F. Bourdreux, Q. Zhang, C. Serre, J.-P. Mahy, N. Steunou, *Angew. Chem., Int. Ed.* **2018**, *57*, 16141; f) P. Li, S.-Y. Moon, M. A. Guelta, S. P. Harvey, J. T. Hupp, O. K. Farha, *J. Am. Chem. Soc.* **2016**, *138*, 8052; g) P. Li, J. A. Modica, A. J. Howarth, E. Vargas, P. Z. Moghadam, R. Q. Snurr, M. Mrksich, J. T. Hupp, O. K. Farha, *Chem* **2016**, *1*, 154.

[7] a) A. P. Côté, A. I. Benin, N. W. Ockwig, M. O'Keeffe, A. J. Matzger, O. M. Yaghi, *Science* **2005**, *310*, 1166; b) X. Feng, X. Ding, D. Jiang, *Chem. Soc. Rev.* **2012**, *41*, 6010; c) S.-Y. Ding, W. Wang, *Chem. Soc. Rev.* **2013**, *42*, 548; d) Y. Jin, Y. Hu, W. Zhang, *Nat. Rev. Chem.* **2017**, *1*, s41570; e) R. P. Bisbey, W. R. Dichtel, *ACS Cent. Sci.* **2017**, *3*, 533; f) F. Beuerle, B. Gole, *Angew. Chem., Int. Ed.* **2018**, *57*, 4850; g) G. Lin, H. Ding, D. Yuan, B. Wang, C. Wang, *J. Am. Chem. Soc.* **2016**, *138*, 3302; h) N. Huang, P. Wang, D. Jiang, *Nat. Rev. Mater.* **2016**, *1*, 16068; i) Y. Song, Q. Sun, B. Aguila, S. Ma, *Adv. Sci.* **2019**, *6*, 1801410; j) S. Kandambeth, K. Dey, R. Banerjee, *J. Am. Chem. Soc.* **2019**, *141*, 1807.

[8] a) S.-Y. Ding, J. Gao, Q. Wang, Y. Zhang, W.-G. Song, C.-Y. Su, W. Wang, *J. Am. Chem. Soc.* **2011**, *133*, 19816; b) Q. Sun, B. Aguila, J. A. Perman, N. Nguyen, S. Ma, *J. Am. Chem. Soc.* **2016**, *138*, 15790; c) X. Wang, X. Han, J. Zhang, X. Wu, Y. Liu, Y. Cui, *J. Am. Chem. Soc.* **2016**, *138*, 12332; d) P. Pachfule, A. Acharjya, J. Roeser, T. Langenhahn, M. Schwarze, R. Schomäcker, A. Thomas, J. Schmidt, *J. Am. Chem. Soc.* **2018**, *140*, 1423; e) H. Liu, J. Chu, Z. Yin, X. Cai, L. Zhuang, H. Deng, *Chem* **2018**, *4*, 1696.

[9] a) G. H. V. Bertrand, V. K. Michaelis, T.-C. Ong, R. G. Griffin, M. Dincă, *Proc. Natl. Acad. Sci. USA* **2013**, *110*, 4923; b) M. Calik, F. Auras, L. M. Salonen, K. Bader, I. Grill, M. Handloser, D. D. Medina, M. Dogru, F. Löbermann, D. Trauner, A. Hartschuh, T. Bein, *J. Am. Chem. Soc.* **2014**, *136*, 17802.

[10] Q. Sun, B. Aguila, J. Perman, L. Earl, C. Abney, Y. Cheng, H. Wei, N. Nguyen, L. Wojtas, S. Ma, *J. Am. Chem. Soc.* **2017**, *139*, 2786.

[11] a) K. Dey, M. Pal, K. C. Rout, S. Kunjattu, A. Das, R. Mukherjee, U. K. Kharul, R. Banerjee, *J. Am. Chem. Soc.* **2017**, *139*, 13083; b) S. Kandambeth, B. P. Biswal, H. D. Chaudhari, K. C. Rout, H. S. Kunjattu, S. Mitra, S. Karak, A. Das, R. Mukherjee, U. K. Kharul, R. Banerjee, *Adv. Mater.* **2017**, *29*, 1603945.

[12] a) Y. Zeng, R. Zou, Y. Zhao, *Adv. Mater.* **2016**, *28*, 2855; b) Y. Pramudya, J. L. Mendoza-Cortes, *J. Am. Chem. Soc.* **2016**, *138*, 15204; c) H. Ma, B. Liu, B. Li, L. Zhang, Y.-G. Li, H.-Q. Tan, H.-Y. Zang, G. Zhu, *J. Am. Chem. Soc.* **2016**, *138*, 5897; d) S. Wang, Q. Wang, P. Shao, Y. Han, X. Gao, L. Ma, S. Yuan, X. Ma, J. Zhou, X. Feng, B. Wang, *J. Am. Chem. Soc.* **2017**, *139*, 4258; e) G.-H. Ning, Z. Chen, Q. Gao, W. Tang, Z. Chen, C. Liu, B. Tian, X. Li, K. P. Loh, *J. Am. Chem. Soc.* **2017**, *139*, 8897; f) X. Han, J. Huang, C. Yuan, Y. Liu, Y. Cui, *J. Am. Chem. Soc.* **2018**, *140*, 892.

[13] a) Q. Fang, J. Wang, S. Gu, R. B. Kaspar, Z. Zhuang, J. Zheng, H. Guo, S. Qiu, Y. Yan, *J. Am. Chem. Soc.* **2015**, *137*, 8352; b) S. Kandambeth, V. Venkatesh, D. B. Shinde, S. Kumari, A. Halder, S. Verma, R. Banerjee, *Nat. Commun.* **2015**, *6*, 6786; c) Y. Peng, Y. Huang, Y. Zhu, B. Chen, L. Wang, Z. Lai, Z. Zhang, M. Zhao, C. Tan, N. Yang, F. Shao, Y. Han, H. Zhang, *J. Am. Chem. Soc.* **2017**, *139*, 8698; d) G. Zhang, X. Li, Q. Liao, Y. Liu, K. Xi, W. Huang, X. Jia, *Nat. Commun.* **2018**, *9*, 2785.

[14] Q. Sun, C.-W. Fu, B. Aguila, J. A. Perman, S. Wang, H.-Y. Huang, F.-S. Xiao, S. Ma, *J. Am. Chem. Soc.* **2018**, *140*, 984.

[15] a) G. Zhang, M. Tsujimoto, D. Packwood, N. T. Duong, Y. Nishiyama, K. Kadota, S. Kitagawa, S. Horike, *J. Am. Chem. Soc.* **2018**, *140*, 2602; b) C. Zhang, X. Wang, M. Hou, X. Li, X. Wu, J. Ge, *ACS Appl. Mater. Interfaces* **2017**, *9*, 13831; c) P. Li, Q. Chen, T. C. Wang, N. A. Vermeulen, B. L. Mehdi, A. Dohnalkova, N. D. Browning, D. Shen, R. Anderson, D. A. Gómez-Gualdrón, F. M. Cetin, J. Jagiello, A. M. Asiri, J. F. Stoddart, O. K. Farha, *Chem* **2018**, *4*, 1022.

[16] a) Z.-F. Pang, S.-Q. Xu, T.-Y. Zhou, R.-R. Liang, T.-G. Zhan, X. Zhao, *J. Am. Chem. Soc.* **2016**, *138*, 4710; b) L. Ascher, T. Sick, J. T. Margraf, S. H. Lapidus, M. Calik, C. Hettstedt, K. Karaghiosoff, M. Döblinger, T. Clark, K. W. Chapman, F. Auras, T. Bein, *Nat. Chem.* **2016**, *8*, 310.

[17] P. Adlercreutz, *Chem. Soc. Rev.* **2013**, *42*, 6406.

[18] V. S. Vyas, M. Vishwakarma, I. Moudrakovski, F. Haase, G. Savasci, C. Ochsenfeld, J. P. Spatz, B. V. Lotsch, *Adv. Mater.* **2016**, *28*, 8749.

[19] F. Haase, E. Troschke, G. Savasci, T. Banerjee, V. Duppel, S. Dörfler, M. M. J. Grundei, A. M. Burow, C. Ochsenfeld, S. Kaskel, B. V. Lotsch, *Nat. Commun.* **2018**, *9*, 2600.

[20] a) J. Liu, S. Bai, Q. Jin, H. Zhong, C. Li, Q. Yang, *Langmuir* **2012**, *28*, 9788; b) R. D. Schmid, R. Verger, *Angew. Chem., Int. Ed.* **1998**, *37*, 1608; c) S. Jung, S. Park, *ACS Catal.* **2017**, *7*, 438.

[21] a) H. Q. Gu, Y. J. Jiang, L. Y. Zhou, J. Gao, *Energy Environ. Sci.* **2011**, *4*, 1337; b) A. Bajaj, P. Lohan, P. N. Jha, R. Mehrotra, *J. Mol. Catal. B: Enzym.* **2010**, *62*, 9; c) L.-H. Liu, Y.-H. Shih, W.-L. Liu, C.-H. Lin, H.-Y. Huang, **2017**, *10*, 1364; d) L. F. Bautista, G. Vicente, Á. Mendoza, S. González, V. Morales, *Energy Fuels* **2015**, *29*, 4981; e) J.-S. Bae, E. Jeon, S.-Y. Moon, W. Oh, S.-Y. Han, J. H. Lee, S. Y. Yang, D.-M. Kim, J.-W. Park, *Angew. Chem., Int. Ed.* **2016**, *55*, 11495.